Proceedings of the 28th IEEE
EMBS Annual International Conference
New York City, USA, Aug 30-Sept 3, 2006

Time-Variant Analysis of Nonlinear Stability and Bispectral Measures to Quantify the Development of Fetal Sleep States

Karin Schwab, Tobias Groh, Matthias Schwab, and Herbert Witte

***Abstract*—A combined time-variant analysis of nonlinear stability and parametric bispectral measures was applied to the *in utero* electrocorticogram (ECoG) of fetal sheep between 0.7 and 0.9 gestation to examine the maturation of sleep states and synchronization patterns of the ECoG. Cycling of the nonlinear stability of the fetal ECoG occurred already at 0.7 gestation and suggests the presence of premature sleep states. This was accompanied by cycling of the time-variant biamplitude which reflected ECoG synchronization effects during premature NREM sleep. Maturation of NREM sleep begun at 0.78 gestation and preceded that of REM sleep that begun at 0.85 gestation. Our results suggest that maturation of brain stem and thalamic function precedes that of cortical function.**

I. Introduction

The development of sleep states is a fundamental event in the maturation of brain function. Yet the time-course of the genesis of sleep states still remains unclear [1]. Sleep states in the mature human fetus are divided into quiet (NREM) sleep and active (REM) sleep accompanied by a state of quiet alertness, and an awake state [2]. NREM and REM periods become first distinguishable between 28 and 31 weeks of gestation according to the appearance of rapid eye movements [3], and fully organized fetal sleep states can be identified from 36 weeks of gestation [2]. Cyclic electrocortical activity alternating between a high-voltage, slow frequency ECoG associated to NREM sleep and a low-voltage, high frequency ECoG associated to REM sleep is a major indicator of differentiation in the development of fetal sleep states. Because of the possibility of an *in utero* instrumentation the chronically instrumented fetal sheep have become the preferred species to study fetal brain activity. Similar to the human fetus, cyclic electrocortical activity can be detected from approximately 0.75 gestation (115 days gestational age - dGA, term 150 dGA) onwards [4]. Using time-variant nonlinear stability and time-invariant direct bispectral analyis [5], we could show continuous functional development of electrocortical activity in both NREM and REM sleep after the emergence of cycling ECoG activity.

This work was supported by DFG Wi 1166/2-3/4, DFG Vo 683/2-1, the Max Kade Foundation and BMBF 01ZZ0105.

K. Schwab and H. Witte are with the Institute of Medical Statistics, Computer Sciences and Documentation, Friedrich Schiller University Jena, 07740 Jena, Germany (corresponding author to provide phone: +49-3641-934131; fax: +49-3641-933200; e-mail: iks@imsid.uni-jena.de).

T. Groh and M. Schwab are with the Department of Neurology, Friedrich Schiller University Jena, 07740 Jena, Germany. (e-mail: Matthias.Schwab@med.uni-jena.de).

The aim of the present study was 1.) to examine the developmental changes of the fetal ECoG that lead to the occurrence of cyclic electrocortical activity, 2.) to adapt a combined use of time-variant nonlinear stability [6]-[8] and time-variant parametric bispectral measure [9] that enabled a continuous and coinstantaneous examination regarding maturation of the ECoG synchronization during NREM sleep, and 3.) to test for the presence of nonlinearities in the fetal ECoG before the emergence of sleep states. The time-variant nonlinear stability analysis has been successfully used in earlier studies of the fetal ECoG investigating different sleep and arousal patterns [5], [7]. Time-variant parametric bispectral analysis which quantifies the occurrence of nonlinear phase couplings between certain frequency components has already been used to quantify the rhythmicity of quadratic phase couplings in the trace alternant EEG of healthy neonates during NREM sleep [10].

II. Material and Methods

A. Surgical instrumentation and experimental protocol

Seven pregnant sheep underwent Caesarian section for fetal instrumentation at 100 dGA. Electrodes were implanted, and fetal ECoG and uterine electromyogram (EMG) to recognize ECoG artifacts due to uterine contractures were recorded continuously from the unanaesthetized fetus over 24 h from 106 to 136 dGA (0.7 to 0.9 gestation). ECoG and EMG signals were amplified, filtered (ECoG 0.5 - 100 Hz, EMG 1-10 Hz) and digitized using a 16 channel A/D board. ECoG was sampled at 128 Hz and EMG at 16 Hz.

B. Data analysis

Data were analyzed at 11 days between 106 and 136 dGA. Starting with 106 dGA, if behaviorally defined sleep states and cycling ECoG activity were not yet detectable by visual analysis of the original ECoG traces, six artifact-free 10 min epochs from each fetus recorded in the early morning hours were chosen randomly. After emergence of cyclic ECoG activity in the original ECoG traces at 118 dGA, we chose six artifact-free 10 min ECoG epochs of REM and NREM sleep, respectively, from each fetus. Additionally, one 60 min epoch was chosen per fetus at 106, 112 and 130 dGA.

For power spectral analysis, the ECoG was quantified continuously in 4 s summaries over 10 min. Fast Fourier Transformation was utilized to evaluate the spectral edge

frequency (SEF) of the total band (1.5-30 Hz) as a sensitive spectral measure [11]. SEF is defined as the frequency below which 95% of the power resides.

For nonlinear stability and bispectral analysis, the data were filtered and sampled down to 64 Hz. Stability analysis was performed by calculating point prediction errors (PPE) of all ECoG epochs for each time point, the received time series were smoothed over 4 s (see chapter 2C). Bispectral analysis was performed by estimating the AR-parameters and the time-variant parametric biamplitude (BA) of the 60 min ECoG eopchs for each time point *t*. A frequency resolution of 0.25 Hz was used. Time-variant mean biamplitudes (tBA) in the region of interest (ROI) F_1xF_2 were examined for F_1=[1.5 Hz ,3 Hz] and F_2=[4 Hz, 8 Hz] (see chapter 2D).

Before the emergence of cyclic ECoG activity in the original ECoG traces, ECoG epochs were defined according to the cycling PPE. Periods with a PPE at least 5% higher than the average PPE of the respective ECoG epoch were defined as REM sleep and periods with a PPE at least 10% lower than the average PPE as NREM sleep (see threshold in Fig 1C). All remaining ECoG periods were left indetermined. The SEF and PPE of the respective NREM and REM sleep ECoG periods in the ECoG epochs were averaged at each gestational age (mean SEF – mSEF, mean PPE - mPPE). The length of the sleep states was determined.

C. Time-variant nonlinear stability analysis

Based on the approach of Takens [12] the measured one-dimensional ECoG $\{x(t_i)\}_{i=1,\ldots,n}$ was transformed into a multi-dimensional phase space by means of a time delay according to

$$Y(t_i) = \{x(t_i), x(t_i - \tau), \ldots, x(t_i - (D_e - 1)\cdot\tau)\} \quad (1)$$

where t_i is the actual time point, τ is the time delay, D_e ist the embedding dimension, and $\{Y(t_i)\}_{i=(De-1)\tau,\ldots,n}$ is the trajectory in the phase space.

The stability analysis is based on the approach of Wolf [8] for the estimation of the leading Lyapunov exponent, but we measured the local exponential divergence of trajectories in the phase space similar to the approach of Gao [6] who did not evaluate single time points but short-time windows. In our approach the nearest Euclidean neighbor have to be searched for each point $y(t_i)$ on a trajectory in the phase space. Changes in the distance of those points were evaluated after evolving a specific time step by

$$PPE_i = \frac{f}{k}\log_2\frac{D'(t_i + k)}{D(t_i)} \quad (2)$$

where t_i is the actual time point, $D(t_i)$ the smallest distance at the time point t_i, $D'(t_i+k)$ the evolved distance at time point t_i+k , k the evolved time steps, f the sampling frequency, and $\{PPE_i\}_{i=(De-1)\tau,\ldots,n-k}$ the resulting time series of point prediction errors (PPE). Equation (2) reflects the degree of stability of any time point in relation to its initial condition. A positive PPE is equivalent to a divergence of neighboring points in the phase space and represents a low stability, a negative or equal to zero PPE describes a quasiperiodic/periodic process or convergence in the phase space and represents a high stability. Numerical values of the PPE are highly dependent on the choice of parameters. We used an embedding dimension of 16, a time delay of 150 ms, an evolving time of 75 ms, and data length of 38400 (10 min) or 230400 (60 min) for our evaluation [8].

D. Time-variant parametric bispectral analyis

To calculate higher order spectra, the transfer function of an estimated AR filter can be applied [13]. Let $\boldsymbol{x}$ be our ECoG signal $(x_1,\ldots,x_n)$ which is to be modelled by $\boldsymbol{y}$. Considering time-series with varying spectral properties, the coefficients of an AR process of order p can be assumed to be time-dependent according to

$$y(t) = \sum_{i=1}^{p} a_i(t)\cdot y(t-i) + e(t). \quad (3)$$

Let $H(f,t)$ be the transfer function of the estimated AR filter of $\boldsymbol{x}$ at the time-point t. The time-variant parametric bispectrum (BS) and biamplitude (BA) occur as

$$\begin{aligned} BS(f_1,f_2,t) &= H\{x\}(f_1,t)\cdot H\{x\}(f_2,t)\cdot H*\{x\}(f_1+f_2,t) \\ BA(f_1,f_2,t) &= |tBS(f_1,f_2,t)|. \end{aligned} \quad (4)$$

The unknown time-variant transfer functions were estimated using an approach of Swami [14] where a so-called instrumental variable

$$z(t) = x(t)\cdot x(t-\tau) \quad (5)$$

was adapted (τ = time delay) which takes into account moments of higher order [15]. The adaptive estimation of the time variant parameter vector

$$\mathbf{a}_p(t) = \left[1, -\mathbf{w}(t)\right]^T = \left[1, -\left(w_1(t),\ldots, w_p(t)\right)\right] \quad (6)$$

of model order p is performed by

$$\mathbf{w}(t) = \mathbf{w}(t-1) + \mathbf{g}(t)\cdot\beta(t) \quad (7)$$

with

$$\begin{aligned} \mathbf{g}(t) &= \frac{\lambda^{-1}\mathbf{P}(t-1)\mathbf{z}(t)}{1+\lambda^{-1}\mathbf{x}^T(t)\mathbf{P}(t-1)\mathbf{z}(t)}, \\ \beta(t) &= d(t) - \mathbf{w}^T(t-1)\mathbf{x}(t), \\ \mathbf{P}(t) &= \lambda^{-1}\mathbf{P}(t-1) - \lambda^{-1}\mathbf{g}(t)\mathbf{x}^T(t)\mathbf{P}(t-1), \end{aligned} \quad (8)$$

where $\boldsymbol{g(t)}$ denotes the gain vector, $\boldsymbol{w(t)}$ the weight vector, λ the forgetting factor ($0<\lambda<1$), $\boldsymbol{P(t)}=\Phi^{-1}(t)$, where $\Phi(t)$ is the correlation matrix of $\boldsymbol{x}$, and $\beta(t)$ specifies the a priori prediction error. The required signal is $d(t)=x(t+1)$, $\boldsymbol{x(t)}$ is the observed signal, and $\boldsymbol{z(t)}$ the instrumental variable. The initial values are $w(0)=0$ and $\boldsymbol{P(0)}=\delta^{-1}\boldsymbol{I}$, where δ is a small positive constant. The quality of the estimation depends strongly on the used model order p and the forgetting factor λ. Therefore, in a previous, methodological study [9] simulations were performed to analyze the convergence rate toward the real bispectrum. Objective function was the known theoretical biamplitude of the simulations. A two-dimensional approach of Schloegl [16] was used for the determination of the convergence rate. A model order p=50 and a forgetting factor λ=0.95 was found to be sufficient.

As the result of the time-variant parametric procedure (4), we obtained a three-dimensional estimation of the time-variant $BA(f_1,f_2,t)$. For a one-dimensional representation of

the assumed phase-coupling phenomena, the time-variant mean biamplitude (tBA) in a ROI F_1xF_2 was derived from the time-variant approach by

$$tBA(t) = \underset{f_2 \in F_2}{mean}\left(\underset{f_1 \in F_1}{mean}\left(BA(t_1, t_2, f)\right)\right). \quad (9)$$

E. Simulations

Simulations were performed to test for nonlinearities in the investigated data at 106, 112 and 130 dGA. For the simulation of pure linear properties in the respective ECoG data, an AR model of order p=25 was fitted to the previously identified NREM and REM sleep periods at the defined dGA. The obtained AR parameters were used to simulate the sleep states at the three different gestational ages. White noise as the input signal of the adapted AR model leads to a signal which is statistically adequate to the original ECoG but contains only linear signal characteristics.

F. Statistics

For statistical analysis, we used non-parametric tests since the averaged mSEFs and mPPEs of the ECoG are not normally distributed. Changes of these parameters over the time-course were tested using a one-sided paired sign test ($p<0.05$). Statistical tests were followed by Holm's adjustment [17] to correct for multiple significance levels.

III. Results

Visually, the ECoG did not show cyclic activity between 106 and 115 dGA in any of the fetuses examined (Fig. 1A). Starting at 118 dGA, the typical cycling between a low-voltage, high frequency and a high-voltage, slow frequency ECoG pattern was noted visually in the original ECoG signal revealing development of REM and NREM sleep, respectively (Fig. 1A, 130 dGA is displayed). The linear measure SEF was able to reflect development of cycling ECoG activity from 112 dGA onwards (Fig. 1B). Using the nonlinear PPE and tBA, cycling of ECoG activity was already visible at 106 dGA in all fetuses examined (Fig. 1C-D). Periods with a low PPE reflect developing NREM sleep ECoG as such periods were associated to the high-voltage, slow frequency NREM sleep ECoG later in development

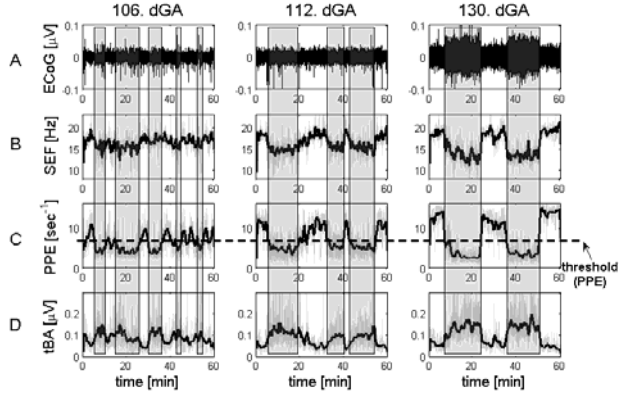

Fig. 1. Examples of 60 min original ECoG epochs at different gestational ages and the related SEF, PPE and tBA in their time course. Periods of developing NREM sleep are indicated (gray bars).

(Fig. 1B-C). Accordingly, periods with a high PPE reflect developing REM sleep ECoG. The developing NREM sleep ECoG was accompanied by a high tBA and the developing REM sleep ECoG by a low tBA revealing the occurrence of nonlinear phase couplings phenomena during developing NREM sleep (Fig. 1C-D). At early ages, the ECoG contained a considerable amount of indetermined epochs that disappeared with advancing gestational age. With advancing gestational age, the sleep states became also more stable (Fig. 1B-D) and their length increased (Table 1).

TABLE I
LENGTH OF SLEEP STATES

dGA	NREM sleep	REM sleep
106	210.69 ± 64.08 s	224.49 ± 76.09 s
112	852.39 ± 101.62 s	1087.26 ± 90.35 s
130	1010.03 ± 87.58 s	1203.96 ± 105.68 s

Developmental changes in the length of developing NREM and REM sleep states evaluated by means of the PPE (mean ± standard deviation in seven fetuses).

The mPPE was higher during the developing REM than during the developing NREM sleep at all gestational ages ($p<0.05$). The mPPE of the developing NREM sleep ECoG was $5.31\pm0.61 s^{-1}$ (mean±SEM) at 106 dGA and decreased to $4.11\pm0.70 s^{-1}$ at 118 dGA ($p<0.05$) suggesting maturation of the NREM sleep. It continued to decline with advancing gestational age to $1.97\pm0.24 s^{-1}$ at 136 dGA ($p<0.05$). The mPPE of the developing REM sleep ECoG was $7.63\pm0.91 s^{-1}$ at 106 dGA. It increased first at 127 dGA to $11.49\pm0.79 s^{-1}$ ($p<0.05$), i.e. later than the mPPE during NREM sleep decreased. The mPPE of the developing REM sleep ECoG continued to increase with advancing gestational age to $14.52\pm0.42 s^{-1}$ at 136. dGA ($p<0.05$).

At 106 dGA, when no cycling in the SEF could be proven the mSEF was 17.01±0.62 Hz. At 112 dGA, the mSEF of the developing REM sleep ECoG was higher than of the developing NREM sleep ECoG (18.55±0.63 Hz *vs.* 16.12±0.66Hz; $p<0.05$). However, the mSEF of the developing NREM sleep ECoG did not change until 118 dGA compared to 112 dGA and decreased from 118 dGA (15.70±0.44 Hz) to 136 dGA (9.60±0.29 Hz, $p<0.05$). The mSEF of the developing REM sleep ECoG did not increase

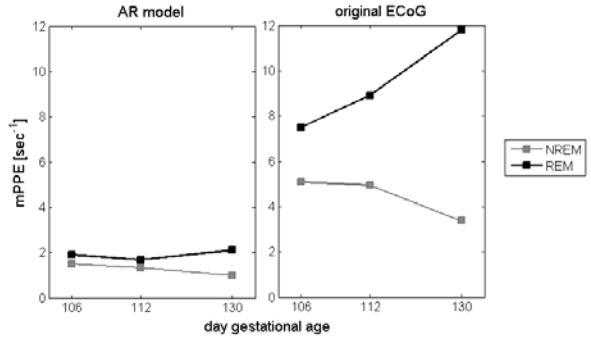

Fig. 2. Comparison of the mPPE of the adapted AR model and of the original ECoG during NREM and REM sleep at 106, 112 and 130 dGA.

until 130 dGA (20.46±0.33 Hz *vs.* 17.01±0.62 Hz at 106 dGA; $p<0.05$), and thus, increased substantially later than in the developing NREM sleep. Again, the mSEF continued to increase to 21.90±0.23 Hz Hz at 136 dGA ($p<0.05$).

The comparison of the mPPE of the adapted AR model and of the ECoG signal revealed the presence of nonlinear portions in the fetal ECoG already at 106 dGA. The mPPE of the AR model was lower then the mPPE of the ECoG in NREM and REM sleep at all gestational ages examined ($p<0.05$, Fig. 2).

IV. Discussion

The aim of the study was to investigate the development of fetal sleep states by a combined time-variant and nonlinear evaluation of the *in utero* ECoG of fetal sheep. Our approach showed the existence of premature sleep patterns already at 0.7 gestation (106 dGA). This suggests functioning of sleep state change inducing neuronal brain stem circuits at this age. The function of these circuits developed over the gestational ages examined (0.7 to 0.9 gestation) as the sleep states became more stable. The nonlinear stability was the most sensitive measure of sleep state development. Its sensitivity can possibly be explained by the presence of nonlinear signal portions that we have shown already at 0.7 gestation. The cycling of the nonlinear stability occurred before the development of cyclic changes of the ECoG frequency spectrum and could be already shown at 0.7 gestation. The high nonlinear stability accompanied by higher biamplitudes in the developing NREM and low nonlinear stability accompanied by lower biamplitudes in the developing REM sleep ECoG reveals nonlinear phase coupling phenomena during NREM sleep and poor organization of the rhythmic pattern during REM sleep. The time-variant bispectral analysis was superior to time-invariant examinations used in an earlier study [5] where phase couplings could be shown only at nearly 0.9 gestation (130 dGA). This is probably due to short term changes in the bispectrum. Therefore, phase couplings cannot be detected by time-invariant approaches.

Interestingly, NREM sleep ECoG activity begun to mature at 118 dGA, i.e. before REM sleep ECoG activity. The development of synchronized slow wave ECoG activity reflects a hallmark of the maturation of integrative functional brain activity. During NREM sleep, the cortical neuronal activity is driven by the regular activity of thalamic nuclei [18]. Interaction of cortical and thalamic networks results in a coordinated occurrence of corticothalamocortical rhythms appearing as slow waves (< 1 Hz), delta waves (1.5-4 Hz) and spindle waves (7-14 Hz) in the ECoG [19]. During REM sleep, the various slow thalamocortical rhythms are inhibited by the tonic input of excitatory impulses from the brain stem [18]. ECoG activity is generated by cortical networks [18], [19]. Thus, it is highly likely that maturation of thalamic pacemaker circuits that mediate synchronized cortical activity precedes maturation of cortical function. The continuous gain of low frequencies and nonlinear stability during NREM sleep after 118 dGA reflects the loss of irregularities in NREM sleep ECoG activity with advancing gestational age. Similarly, complex cortical ECoG activity during REM sleep preceded to mature after it developed at 127 dGA. In conclusion, the combined time-variant application of nonlinear stability and parametric bispectral measure provides important insights in the collective behavior of the neural networks during the developing of organized sleep states.

References

[1] D. McGinty and R. Szymusiak, "The sleep-wake switch: A neuronal alarm clock," *Nat. Med.*, vol. 6, pp. 510-1, 2000.

[2] J. G. Nijhuis, H. F. Prechtl, C. B. Martin, Jr., and R. S. Bots, "Are there behavioural states in the human fetus?," *Early Hum. Dev.,* vol. 6, pp. 177-95, 1982.

[3] T. Okai, S. Kozuma, N. Shinozuka, Y. Kuwabara, and M. Mizuno, "A study on the development of sleep-wakefulness cycle in the human fetus," *Early Hum. Dev*., vol. 29, pp. 391-6, 1992.

[4] H. H. Szeto and D. J. Hinman, "Prenatal development of sleep-wake patterns in sheep," *Sleep*, vol. 8, pp. 347-55, 1985.

[5] K. Schmidt, M. Kott, T. Muller, H. Schubert, and M. Schwab, "Developmental changes in the complexity of the electrocortical activity in foetal sheep," *J. Physiol. Paris*, vol. 94, pp. 435-43, 2000.

[6] J. B. Gao and Z. M. Zheng, "Direct Dynamical Test for Deterministic Chaos and Optimal Embedding of a Chaotic Time-Series," *Phys. Rev. E*, vol. 49, pp. 3807-3814, 1994.

[7] M. Schwab, K. Schmidt, H. Witte, and M. Abrams, "Investigation of nonlinear ECoG changes during spontaneous sleep state changes and cortical arousal in fetal sheep," *Cereb. Cortex*, vol. 10, pp. 142-8, 2000.

[8] A. Wolf, J. B. Swift, H. L. Swinney, and J. A. Vastano, "Determining Lyapunov Exponents from a Time-Series," *Physica D*, vol. 16, pp. 285-317, 1985.

[9] K. Schwab, M. Eiselt, C. Schelenz, and H. Witte, "Time-variant parametric estimation of transient quadratic phase couplings during electroencephalographic burst activity," *Methods Inf. Med*., vol. 44, pp. 374-383, 2005.

[10] K. Schwab, P. Putsche, M. Eiselt, M. Helbig, and H. Witte, "On the rhythmicity of quadratic phase coupling in the trace alternant EEG in healthy neonates," *Neurosci. Lett*., vol. 369, pp. 179-82, 2004.

[11] H. H. Szeto, T. D. Vo, G. Dwyer, M. E. Dogramajian, M. J. Cox, and G. Senger, "The ontogeny of fetal lamb electrocortical activity: a power spectral analysis," *Am. J Obstet. Gynecol*., vol. 153, pp. 462-6, 1985.

[12] F. Takens, "Detecting strange attractors in turbulence," in *Dynamical systems in turbulence*, D. Rand and L. S. Young, Eds. New York: Springer, 1981, pp. 366-381.

[13] L. Nikias and A. P. Petropulu, *Higher-order spectra analysis - a nonlinear signal processing framework*. New Jersey: Prentice Hall, 1993.

[14] A. Swami, "System identification using cumulants," in *Thesis*: University of Southern California, 1988.

[15] P. Stoica, T. Soderstrom, and B. Friedlander, "Optimal Instrumental Variable Estimates of the AR Parameters of an ARMA Process," *IEEE Trans. Autom. Control*, vol. 30, pp. 1066-1074, 1985.

[16] A. Schloegl, *The electroencephalogram and the adaptive autoregressive model: theory and applications*. Aachen: Shaker, 2000.

[17] S. Holm, "A simple sequentially rejective multiple testing procedure," *Scand. J. Statistics*, vol. 6, pp. 65-70, 1979.

[18] D. A. McCormick and T. Bal, "Sleep and arousal: thalamocortical mechanisms," *Annu. Rev. Neurosci*., vol. 20, pp. 185-215, 1997.

[19] M. Steriade, F. Amzica, and D. Contreras, "Cortical and thalamic cellular correlates of electroencephalographic burst-suppression," Electroencephalogr. *Clin. Neurophysiol*., vol. 90, pp. 1-16, 1994.